J Therm Anal Calorim (2010) 102:627–632
DOI 10.1007/s10973-010-0837-2

Non-isothermal kinetics of melting and nematic to isotropic phase transitions of 5CB liquid crystal

Dipti Sharma

NATAS2009 Special Issue

Abstract This work reports a non-isothermal kinetics of the melting and the nematic to isotropic (N–I) phase transitions of the pentylcyanobiphenyl (5CB) liquid crystal compared with octylcyanobiphenyl (8CB) liquid crystal using calorimetric technique. Temperature scans and heating rate scans were performed for 5CB and 8CB from 280 to 333 K at various rates using differential scanning calorimetry from 0.5 to 20 K min^{-1}. Double activation was observed for 5CB for two heating rate regimes whereas 8CB indicated single activation only. The 5CB has smaller enthalpy and entropy of the transitions and needs larger activation than 8CB. This kinetic change can be explained in terms of the length scale and mobility of the liquid crystal molecules.

Keywords Calorimetry · Liquid crystals · Nematic to isotropic phase transition · Kinetics · Heat capacity

Introduction

Among the great scientific and technological achievements of the twentieth century, the integrated electronics and liquid crystal displays in combination with the portable computing revolution need more information about the behavior of phase transitions of the *n*-cyanobiphenyl (*n*CB) liquid crystals [1–11]. As we enter the twenty first century, the study of the liquid crystals offers unparalleled opportunities to advance the basic science and materials design of condensed matter, and to develop new liquid crystal applications, which lead the researchers and scientists to explore more the hidden behavior of the phase transitions of the liquid crystals [1–5].

Liquid crystal pentylcyanobiphenyl (5CB) and octylcyanobiphenyl (8CB) are the materials of interest in research due to their proto-typical thermotropic nature in nematic to isotropic (N–I) phase transition and have been studied by various authors as a host material to form clay and polymer composites, solvent additives, and liquid crystal mixtures by X-ray diffraction, FTIR, optical microscopy, dielectric spectroscopy, and calorimetry techniques for several years [5–8]. Some reports can be seen on bulk 5CB and 8CB to discuss the effect of anapore membranes, vycor glass, and temperature variation on (N–I) phase transition [8–11], but no reports have been found on the kinetics of the melting transition and N–I phase transition of the 5CB liquid crystal so far and make this study important in the field of the liquid crystal research. Furthermore, the phase transition dynamics can also be studied in the form of energy required or gained by the liquid crystal molecules during the transition depending upon heating rate kinetics. Some of our publications have focused on heating rate dynamics of the aligned and unaligned bulk 8CB liquid crystal to show the importance of the kinetics of the aligned liquid crystals [12–17].

Here, the present article reports a non-isothermal activated kinetics to show the requirement of double activation for the melting and N–I phase transitions of 5CB liquid crystal. This activated kinetics shows a drastic change occurred in the kinetics of the 5CB liquid crystal when compared with the kinetic results of its close family member of 8CB liquid crystal.

D. Sharma (✉)
University of Massachusetts Lowell, Lowell, MA 01854, USA
e-mail: dr_dipti_sharma@yahoo.com

Experimental details

Bulk 4-pentyl-4-cyanobiphenyl (5CB) and 4-octyl-4-cyanobiphenyl (8CB) liquid crystals were obtained from Frinton Laboratories, having molecular weight 249.36 and 291.44, respectively. They were degassed for about 1 h under a vacuum unit at room temperature 293 K and then used to study. For calorimetric experiments, the sample of 5CB and 8CB were loaded for heating scans into a differential scanning calorimeter (DSC-TA instruments) to obtain DSC thermograms of the samples at various heating ramp rates. The sample was first annealed at 323 K for 5 min then cooled to 280 K and equilibrated for 15 min, then heating scans were performed from 280 to 333 K at the rate of 5 K/min. Same heating scan experiments were also performed at different heating ramp rates varying ramp rates from 0.5 to 20 K min^{-1} keeping other conditions same to get a comparison between heating rate results. The DSC instrument was well calibrated before the start of each run of the experiments. The respective heat flow of the samples was recorded along with temperature change during the heating scans. All environmental and experimental conditions were kept identical for all runs so that a good comparison of the transitional parameters could be made to understand the kinetics of the melting and the N–I transition of the 5CB and 8CB liquid crystals.

Results and discussion

In the heating scans, well-defined endothermic peak was observed for the melting and the nematic to isotropic (N–I) phase transition for 5CB and 8CB liquid crystals at 296 K and 294.4 K for melting, and at 307.3 K and 313.2 K for N–I with 5 K min^{-1} ramp rate, respectively, shown in Fig. 1. In the 5CB, melting transition occurs 1.5 K after the melting transition of 8CB, and the N–I transition occurs 6 K earlier than the N–I transition of 8CB. The size of the transition peaks in 5CB is smaller than the size of the peaks of 8CB. This heat flow was later converted to the specific heat capacity of the samples, shown by Eq. 1 below.

$$dH/dt = \Delta C_p * (dT/dt) \quad (1)$$

where dH/dt, dT/dt, and ΔC_p are the heat flow, heating rate, and the excess of specific heat capacity, respectively.

Figure 2 shows a zoom in part of the N–I phase transition for the 5CB and 8CB liquid crystals where the lower section shows the wing's behavior at the nematic side for both liquid crystals. The N–I transition shows an energy difference between nematic to isotropic state of the liquid crystal molecules by a gap between the wings of the transition on nematic and isotropic states where isotropic state is found to be on higher energy level than nematic

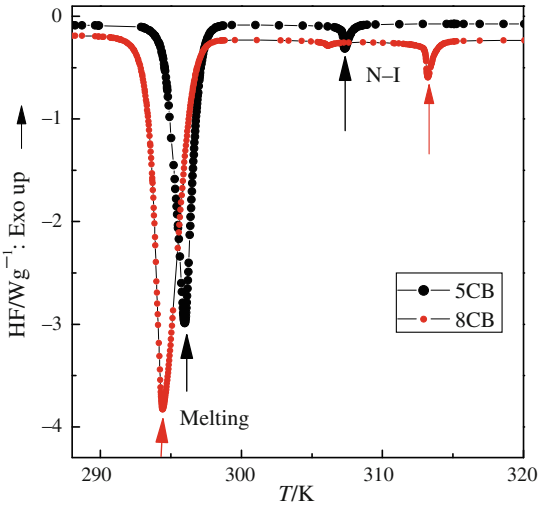

Fig. 1 Heat flow versus temperature plot showing the melting transition and N–I phase transition of the 5CB (*black symbol*) and 8CB (*red symbol*) liquid crystals. (Color figure online)

state. This energy gap ΔH_g can be considered as the energy gained by liquid crystal molecules reaching from nematic to isotropic state during the N–I transition and can be found from the wing gap. The 5CB shows 1.9 times smaller energy gain during the transition than 8CB. The total enthalpy of the N–I transition for 5CB is found 1.4 times smaller than the 8CB. The wing behavior and the energy gap are absent in the melting transition. The enthalpy of the

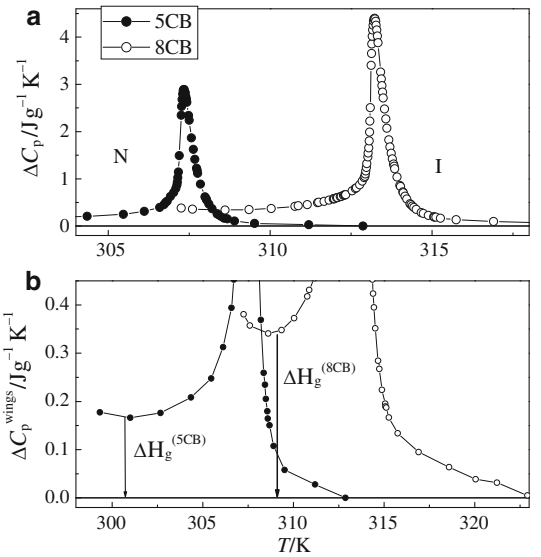

Fig. 2 **a** Temperature dependence of the excess of specific heat capacity versus temperature plot showing N–I phase transition at 307.3 K and 313.2 K with 5 K/min ramp rate for 5CB and 8CB respectively, **b** the excess of specific heat capacity of the nematic wings at the nematic state as a function of temperature for 5CB and 8CB indicating the energy gained by nematic domains during the N–I phase transition in terms of ΔH_g

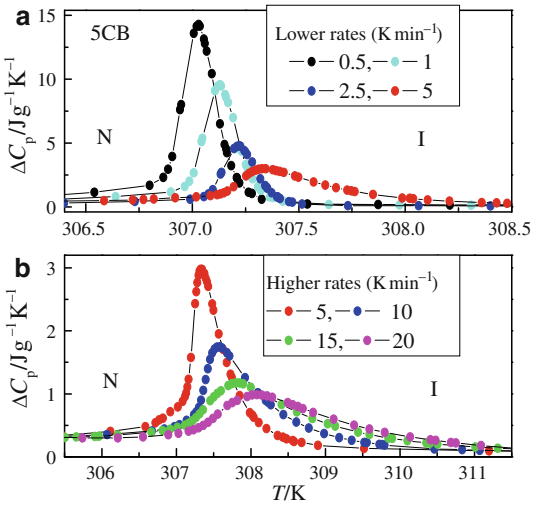

Fig. 3 Heating rate dependence of the N–I phase transition of 5CB liquid crystal as a function of temperature varying the ramp rates from 0.5 to 20 K min^{-1}. **a** Slow shift regime: shift in the transition peak is slower at lower heating rates varying from 0.5 to 5 K min^{-1}, **b** high shift regime: shift of the transition peak is larger at higher heating rates varying from 5 to 20 K min^{-1} rates

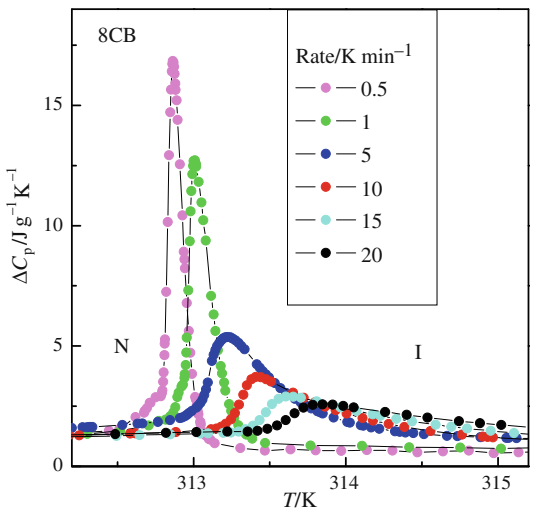

Fig. 4 Heating rate dependence of the N–I phase transition of 8CB liquid crystal as a function of temperature varying ramp rates from 0.5 to 20 K min^{-1}

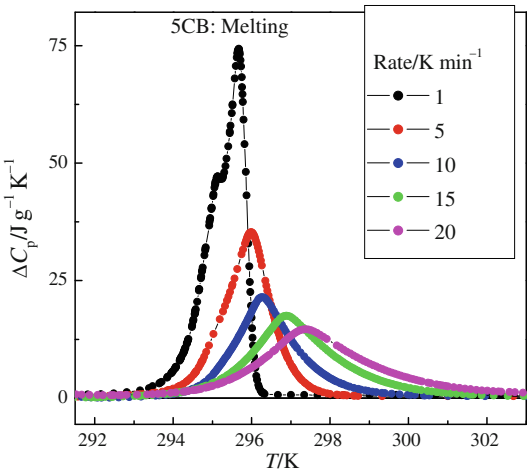

Fig. 5 Heating rate dependence of the melting transition of 5CB varying heating rates from 1 to 20 K min^{-1}. The melting peak at 1 K min^{-1} shows a wider and taller peak with an additional smaller peak indicating a slower crystallization. A slower shift in the peaks can be seen until 5 K min^{-1}. A smooth and faster shift in the transition peak can be seen from 5 to 20 K min^{-1}

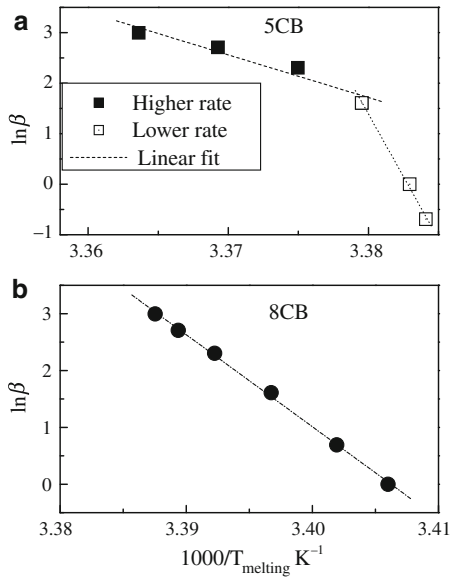

Fig. 6 Arrhenius plot to the melting transition of the 5CB and 8CB: **a** 5CB indicates double activation in terms of two linear sloped where the *filled* and *empty* symbols indicate higher (from 20 to 5 K min^{-1}) and lower (from 5 to 0.5 K min^{-1}) heating rates regimes, respectively. **b** 8CB shows the single activation in terms of one linearity

melting transition of 5CB is 1.2 times smaller than the melting transition of 8CB.

In the heating rate experiments, a temperature shift in the melting and the N–I phase transition peaks were observed towards higher temperature. The trend of temperature shift is found very different in 5CB than 8CB as the heating rate is increased from 0.5 to 20 K min^{-1}. The temperature shift in the melting transition and the N–I phase transition for the 5CB are found slower for the heating rates from 0.5 to 5 K min^{-1} and then becomes faster for the heating rates from 5 to 20 K min^{-1} following two different linear trends whereas 8CB shows a smooth temperature shift with one linearity from 0.5 to 20 K min^{-1} for the melting and N–I transitions. To see the clear temperature shifts in the N–I phase transition peak, Fig. 3 is plotted for the two heating rate regimes separately; one for the lower heating rate regime from 0.5 to 5 K min^{-1} and other for the higher heating rate regime from 5 to 20 K min^{-1}. It is clear from this figure that the

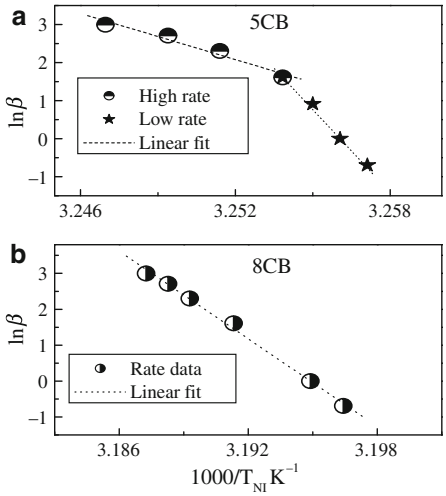

Fig. 7 Arrhenius plot to the N–I phase transition of the 5CB and 8CB liquid crystals: **a** 5CB indicates two linearity for two heating rate regimes where the *filled* and *empty* symbols indicate higher (from 20 to 5 K min^{-1}) and lower (from 5 to 0.5 K min^{-1}) heating rates regimes, respectively. **b** 8CB shows the single activation

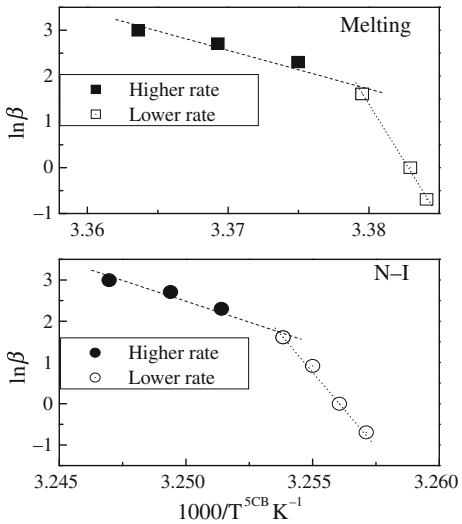

Fig. 8 A comparative Arrhenius plot to the melting and N–I transition of the 5CB liquid crystals. Slopes of the N–I transition are higher than melting transition slopes and indicates higher activation energy for the N–I transition than melting transition for the same heating rates from 0.5 to 20 K min^{-1}

N–I phase transition of 5CB needs two linear fitting for the observed data for these two heating rate regimes whereas the N–I phase transition of 8CB needs only one linear fitting to the data observed for the same heating rate regime range from 0.5 to 20 K min^{-1} rates, shown in the Fig. 4. Heating rate effect can be seen on the melting transition of the 5CB too. The melting peak becomes wider, larger and shows multi-peaks because of slow shift and slow crystallization for the lower heating rates (see the peak at 1 K min^{-1}) as heating rate decreases, shown in Fig. 5. The shifting of the melting peak also follows two different

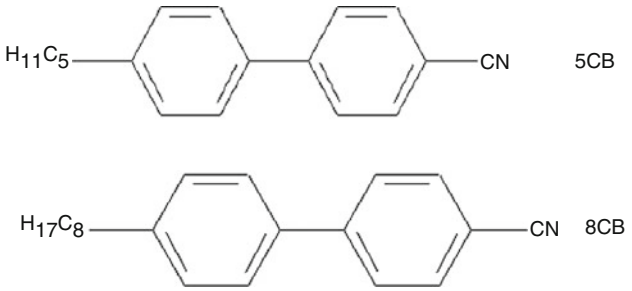

Fig. 9 The molecular structure of 5CB and 8CB liquid crystals having CN, phenyl rings, C–C and C–H groups

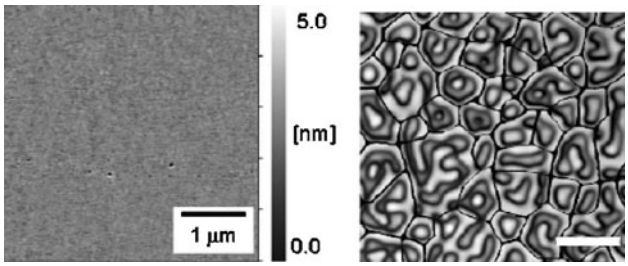

Fig. 10 AFM images of the 5CB (*left*) and 8CB (*right*) liquid crystals at 20 °C and 39 °C showing the nematic domain formation at the nematic states where borders between nematic domains appear as *darker lines* (image taken from the refs. [21, 22]). The scale bar for the left image is 1 μm and for the right image is 100 μm

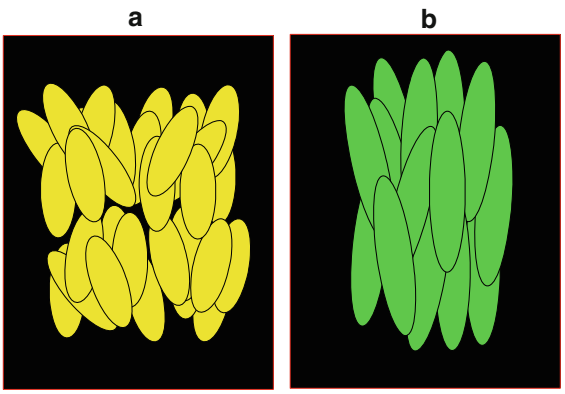

Fig. 11 Cartoon depicting the nematic domain of **a** 5CB and **b** 8CB where the *black background* shows the fixed amount of the liquid crystal and the number of liquid crystal molecules indicates the density showing the formation of the nematic domains. The nematic domain is smaller and denser in the 5CB than 8CB

linearity for two heating rate regimes and becomes slower for the lower heating rate regime and higher for the higher rate regime whereas the melting peak of 8CB follows only one linearity for the same heating rate range from 0.5 to 20 K min^{-1}.

Using Arrhenius theory [18, 19], the activation energy of molecular motion and rearrangement of the 5CB and

Table 1 Data details for the kinetics of the melting and N–I transitions of 5CB

5CB	ΔE_1	ΔE_2	ΔE_{AVE}	ΔH	ΔS	T	ΔH_g
Melting	0.70 (±0.10)	4.12 (±0.10)	2.41 (±0.10)	13.95	47.13	295.98	–
N–I	1.68 (±0.01)	6.02 (±0.02)	3.85 (±0.02)	0.65	2.10	307.35	0.34

Table shows the required activation energy of the transitions at the lower heating rate regime from 0.5 to 5 K min^{-1} (ΔE_1/kJ mol^{-1}), activation energy at the higher rate regime from 5 to 20 K min^{-1} (ΔE_2/kJmol^{-1}), averaged activation energy (ΔE_{AVE}/kJ mol^{-1}) with the standard deviations of the evaluated activation energies in the parenthesis, total enthalpy (ΔH/kJ mol^{-1}), entropy (ΔS/J mol^{-1} K^{-1}), transition temperature (T/K), and energy gain by the nematic domains during the transition (ΔH_g/kJ mol^{-1})

8CB near the transition (melting and N–I) temperature can be found from the following relation:

$$\beta = \beta o \mathrm{Exp}[-\Delta E/RT] \quad (2)$$

where β is the effective heating rate (K min^{-1}), βo is a constant (K min^{-1}), ΔE is the activation energy (J mol^{-1}), R is universal gas constant (J mol^{-1} K^{-1}), and T is the absolute temperature (K). A comparative analysis between 5CB and 8CB liquid crystal reveals that 5CB shows double activation energy where 8CB shows a single activation for the N–I transitions. Figures 6 and 7 show the Arrhenius plot for the melting and the N–I transitions where the upper section shows the 5CB and the lower 8CB results and it is clear that the data points of the melting and the N–I transitions need two linearity whereas 8CB needs only one linear fitting for the same heating rates. Transitions of the 5CB show higher activation energy with smaller enthalpy for the N–I transition than 8CB liquid crystal. Figure 8 shows a comparison between the melting and the N–I transitions of 5CB for the same heating rates. The melting transition absorbs larger energy and hence needs smaller activation energy than the N–I phase transition of the 5CB. These changes in 5CB can be explained in terms of the length scale and the mobility of the liquid crystal molecules.

The length of the 5CB liquid crystal molecule is 1.2 times smaller than 8CB liquid crystal molecule, shown the molecular structure of the liquid crystals in the Fig. 9. The critical distance of the nematic domain of 5CB is 1.6 times smaller than the typical nematic domain length of 8CB [20] and the density of the 5CB at the nematic state is 1.1 times larger than 8CB at the nematic state (density details can be seen on the liquid crystal webpage http://liqcryst.chemie.uni-hamburg.de/lc_lc.php). The AFM image of the nematic domain of 5CB and 8CB (taken from the references [21, 22]) can be seen in the Fig. 10 where the distance of the domain is clearly smaller than the 8CB domain. Because of the smaller size and larger density of 5CB, the number of nematic domains in the fixed amount of liquid crystal is larger than the number of nematic domains of 8CB, shown in Fig. 11, and makes the 5CB liquid crystal molecules less active that reduces the mobility and activity of the 5CB molecules than 8CB molecules. Furthermore, in the lower heating rate regime, the 5CB nematic domains get enough time to undergo to the disordered state but at the higher heating rates, the time given by heating rate to the nematic domains is less than the required and this difference in time forces the transition peak to move faster towards isotropic state in terms of the larger temperature shift. Therefore, the process of the molecular motion and rearrangement of the 5CB molecules near the N–I phase transition indicates two energy requirement for lower (from 0.5 to 5 K min^{-1}) and higher (from 5 to 20 K min^{-1}) heating rate regimes and brings double activation in terms of two slopes during the transition. Due to the smaller size of 5CB molecules, the enthalpy of the melting and the N–I transitions are 1.4 and 1.2 times smaller than 8CB and hence indicates 1.5 and 1.2 times larger energy required in terms of average activation energy during the transition for 5CB molecules. Data details can be seen for the comparative analysis of the activated kinetics of the melting and N–I transitions of the 5CB and 8CB liquid crystals in the given Tables 1, 2 and 3.

Table 2 Data details for the kinetics of the Melting and N–I transitions of 8CB

8CB	ΔE	ΔH	ΔS	T	ΔH_g
Melting	1.59 (±0.10)	26.91	91.41	294.40	–
N–I	3.27 (±0.03)	0.91	2.91	313.20	0.67

Table shows the activation energy of the transitions from 0.5 to 20 K min^{-1} (ΔE/kJ mol^{-1}) with the standard deviations of the evaluated activation energy, total enthalpy (ΔH/kJ mol^{-1}), entropy (ΔS/J $mol^{-1}K^{-1}$), transition temperature (T/K), and energy gain by the nematic domains during the transition (ΔH_g/kJ mol^{-1})

Table 3 A comparative molecular information of 5CB and 8CB liquid crystal molecules

nCB	L	W	ρ	L_d [20]	N^{C-C} and N^{C-H}
5CB	1.5	0.5	1.045	3.2	5, 11
8CB	2	0.5	0.985	2	8, 17

Table shows the length of the molecule (L/nm), width of the molecule (W/nm), specific density of the liquid crystal at the nematic state (ρ/g cm^{-3}), critical distance of the nematic domains (taken from the reference [20]) (L_d [20]/nm), number of C–C and C–H bonds in the tail of the liquid crystal molecules those are responsible to change the length of the molecules (N^{C-C} and $N^{C-H)}$

Conclusions

A non-isothermal kinetic investigation has been made to understand the activated kinetics of the melting transition and the N–I phase transition of 5CB liquid crystal using calorimetric technique. Well defined endothermic peaks were found on heating scans on melting and the N–I transition for the 5CB. These transitions were found to be shifted towards higher temperatures following Arrhenius behavior with two linear trends as heating ramp rate was increased from 0.5 to 20 K min^{-1}. This temperature shift indicated two activation energy requirement for the transitions at lower (0.5–5 K min^{-1}) and higher (5–20 K min^{-1}) heating ramp rate regimes. Single activation energy was required for the transitions for the same experimental and environmental conditions when compared with the 8CB results to see the kinetic changes in two close family members of the *n*CB liquid crystal. The transitions of the 5CB indicated higher activation with smaller enthalpy when compared with the transitions of the 8CB. Since the energy absorbed by the 5CB molecules was smaller during the transition, they needed larger activation than 8CB liquid crystal molecules. This behavior can be explained in terms of the length scale and the mobility of the liquid crystal molecules of 5CB and 8CB.

References

1. Vanbrabant P, Dessaud N, Strömer J. Temperature influence on the dynamics of vertically aligned liquid crystal displays. Appl Phys Lett. 2008;92:091101–3.
2. Samei E. A comparative contrast-detail study of five medical displays. Med Phys. 2008;35:1358–64.
3. Wilk R, Vieweg N. THz spectroscopy of liquid crystals from the CB family. J Infrared Millim Terahertz Waves. 2009;30:1139–47.
4. Liang D, Leheny R. Smectic liquid crystals in an anisotropic random environment. Phys Rev E. 2007;75:031705.
5. Budaszewski D, Domański AW. Depolarization of light in microstructured fibers filled with liquid crystals. Opto Electron Rev. 2009;17:156–60.
6. Gvozdovskyy I, Kurioz Y. Exposure and temperature dependences of contact angle of liquid crystals on photoaligning surface. Opto Electron Rev. 2009;17:116–9.
7. Motosuke M, Nagasaka Y. Real-time sensing of the thermal diffusivity for dynamic control of anisotropic heat conduction of liquid crystals. Int J Thermophys. 2008;29:2025–35.
8. Zakharov AV, Thoen J. Surface-induced smectic-ordering effect in thin nematic liquid-crystal cell. Eur Phys J E. 2002;9:461–6.
9. Iannacchione G, Finotello D. Specific heat dependence on orientational order at cylindrically confined liquid crystal phase transitions. Phys Rev E. 1994;50:4780–95.
10. Iannacchione GS, Crawford GP, Zumer S, Doane JW, Finotello D. Randomly constrained orientational order in porous glass. Phys Rev Lett. 1993;71:2595–8.
11. Mansare T, Decressain R, Gors C, Dolganov VK. Phase transformations and dynamics of 4-cyano-4′-pentylbiphenyl (5CB) by nuclear magnetic resonance, analysis differential scanning calorimetry, and wide angle X-ray diffraction analysis. Mol Cryst Liquid Cryst Sci Technol. 2002;382:97–111.
12. Sharma D. Calorimetric study of activated kinetics of the nematic and smectic phase transitions in an aligned nano-colloidal liquid crystal + aerosil gel. J Therm Anal Calorim. 2008;93:899–906.
13. Sharma D. Kinetics of nanocolloids in the aligned domain of octylcyanobiphenyl and aerosil dispersion. Liquid Cryst. 2008;35:1215–24.
14. Sharma D, Iannacchione GS. Kinetics of induced crystallization of the LC1-*x*Sil*x* system. J Phys Chem B. 2007;111:1916–22.
15. Sharma D, MacDonald JC, Iannacchione GS. Thermodynamics of activated phase transitions of 8CB: DSC and MC calorimetry. J Phys Chem B. 2006;110:16679–84.
16. Sharma D. Effect of alignment on the nematic to isotropic phase transition of bulk octylcyanobiphenyl brings possible solutions to liquid crystal display drawback. Appl Phys Lett. 2009;94:134103.
17. Sharma D, MacDonald JC, Iannacchione GS. Role of aerosil dispersion on the activated kinetics of the LC1-*x*Sil*x* system. J Phys Chem B. 2006;110:26160–9.
18. Vogel H. The law of the relation between the viscosity of liquids and the temperature. Phys Z. 1921;22:645–6.
19. Fulcher GS. Analysis of recent measurements of the viscosity of glasses. J Am Ceram Soc. 1925;8(6):339–55.
20. Jin T, Finotello D. Adsorption-induced anchoring transition in cylindrically confined liquid-crystal hydrophobic aerosil dispersions. Europhys Lett. 2005;69:221–7.
21. Toda A, Nagano S, Seki T. Ideal spread monolayer formation and surface pressure induced orientation in poly(9,9-di-n-octylfluorene-alt-benzothiadiazole) via hybridized with liquid crystal molecule on water. Synth Met. 2009;159:835–8.
22. Schlagowski S, Jacobs K, Herminghaus S. Nucleation-induced undulative instability in thin films of *n*CB liquid crystals. Europhys Lett. 2002;57:519–25.